Weak spatial dispersion and the unfolding of wave arrival singularities in the elastodynamic Green's functions of solids

A. G. Every*
School of Physics, University of the Witwatersrand, P.O. WITS 2050, Johannesburg, South Africa
(Received 12 July 2005; revised manuscript received 4 August 2005; published 22 September 2005)

This paper is concerned with the influence of spatial dispersion on transient acoustic waves in solids, and in particular with how the first onset of spatial dispersion leads to the unfolding of wave arrival singularities into wave trains known as pseudo-wave arrivals. Spatial dispersion is the dependence of wave speed on spatial frequency, and arises when the wavelength approaches the natural length scale of the medium, which might for example be the lattice spacing of a crystal or the repeat distance of a layered solid or fiber composite. In centrosymmetric crystals, which are treated here, the initial onset of spatial dispersion is represented by a correction to the limiting wave speed which is of second order in the spatial frequency, and the augmentation of the wave equation with fourth order spatial derivatives. Using Fourier transform techniques, general formulas are derived here for the line and point force elastodynamic Green's functions of centrosymmetric anisotropic solids subject to weak spatial dispersion. Numerical examples are provided of isotropic solids exhibiting wave arrival singularities, and the analytic forms are established of the pseudo-arrival unfoldings of the step function, delta function and ramp function arrivals of point force Green's functions, and the $1/\sqrt{\tau}$ and $-\sqrt{\tau}$ arrivals of line force Green's functions, where τ is time after arrival.

DOI: 10.1103/PhysRevB.72.104302 PACS number(s): 62.30.+d, 62.65.+k, 43.35.+d

I. INTRODUCTION

The influence of dispersion on the propagation of transient elastic waves in solids is of fundamental interest in solid state physics, materials science, seismology, and other fields. Within the domain of linear elasticity, one distinguishes between temporal and spatial dispersion. Temporal dispersion is the variation of wave speed, v, with frequency, f, and is usually interpreted as a viscoelastic effect, having its origin in time dependent relaxation processes.[1,2] It can also be due to resonant absorption.[3] Spatial dispersion is the variation of wave speed with spatial frequency (wave vector), $\mathbf{k}$, and arises when the wavelength, λ, approaches the natural length scale, Λ, of the medium, which might for example be the lattice spacing in a crystal, or the repeat distance of a layered solid or fibre composite.[4] It is also implicated in sound propagation in granular materials, foams, nanostructures and other complex media.[5] Spatial dispersion has found fertile ground for application recently in the area of picosecond laser ultrasonics.[6] Geometrical dispersion, i.e., the dispersion of guided waves in rods and plates, is also in a sense spatial dispersion, with the length scale being the diameter of the rod or thickness of the plate.[7,8] Sachse and Pao[9] identify the scattering of waves by densely distributed fine inhomogeneities in materials as a source of dispersion, and this too can be regarded as a form of spatial dispersion. Nonlinearity, an important source of dispersion, whereby the wave speed depends on the amplitude of a wave, lies outside the scope of this paper, which is concerned with small amplitude waves.

Both attenuation and dispersion have the effect of spreading out an initially sharp acoustic pulse or wave front. Attenuation, on its own, leads to the simple rounding of the pulse or front. Dispersion, on the other hand, gives rise to a wave train, with ripples trailing (usually) or leading (in some cases) the broadened main arrival.[4,10] The ripples become more narrowly spaced with distance from the main arrival, reflecting the fact that as the pulse or front propagates, its higher (spatial or temporal) frequency Fourier components become progressively separated from the lower frequency components, which are relatively unaffected by dispersion. The effects of spatial dispersion on pulse propagation in 1D (or equivalently plane wave pulse propagation in 3D) are fairly well understood. Theory predicts that an initially sharp delta function $\delta(x)$ pulse will evolve into a waveform conforming to the Airy function $\mathrm{Ai}(x)$, and this has recently been confirmed in a striking way in picosecond laser ultrasound experiments by Hao and Maris.[6] The analogous broadening of a step function pulse in layered composites has been discussed by Christensen[4] and more generally for media with discrete microstructure, by Askes and Metrikine.[11] Kaplunov *et al.*[8] have made an extensive study of the unfolding of wave arrivals in plates into pseudo-wave arrivals under the influence of geometrical dispersion.

This paper is aimed at elucidating the effects of spatial dispersion on sharp features, known as wave arrival singularities, that are present in the elastodynamic Green's functions of three-dimensional solids, and describing how these unfold into oscillatory pseudo-wave arrivals. Specific consideration is given to the effects of weak spatial dispersion on the displacement response of a centrosymmetric solid to a point force with unit step function $\Theta(t)$ time dependence (the 3D Green's function), and to a line force with $\delta(t)$ time dependence (the 2D Green's function).

There are two basic approaches one can take in constructing a continuum elasticity theory that incorporates spatial dispersion. One is to start from a microscopic model for a particular type of solid, and carry out a suitable expansion, in powers of $\mathbf{k}$ say.[12,13] The terms beyond lowest order then represent dispersive corrections to classical continuum elas-

ticity. The other approach, leading to what is termed "generalized continuum elasticity," is to use concepts of a fairly general nature, without reference to any specific microscopic model, to extend classical continuum elasticity into the shorter wavelength dispersive regime. A wealth of information on the subject is to be found in the proceedings of the IUTAM Symposium "Mechanics of Generalized Continua."[14] The latter approach has the advantage of revealing universal features in the elastic behaviour of solids on a short scale, regardless of their particular microscopic nature. As such it is applicable not only to conventional solids, but also to media such as foams and granular materials, where there may not be at hand a microscopic model, except in a statistical sense.

Generalized continuum elasticity theories themselves come in two basic forms (as well as hybrids of the two).[14–16] In Cosserat (micropolar) elasticity, the displacement field of a solid is taken to be comprised of the Cartesian displacement as well as internal rotation of each "particle" of the medium. In the coupling between the displacement and rotational degrees of freedom, a scale of length emerges, and fourth order derivatives enter into the wave equation, rendering it dispersive.[17] The second form, known as gradient or non-local elasticity, assumes the stress-strain relationship to be non-local in form.[18] For wavelengths longer than the range of the kernel of the integral relation between stress and strain, it emerges that the stress at a point depends not only on the displacement gradient at that point, but also on higher spatial derivatives of the displacement field. As a result, spatial derivatives of higher order than second appear in the wave equation, rendering it dispersive. A Lagrangian approach leads to the same conclusion, but arguably from a more systematic and rigorous foundation.[19]

In this paper the effects of spatial dispersion on transient wave propagation are treated within the context of gradient elasticity. The first stage of the analysis is formulated for centrosymmetric, but otherwise generally anisotropic solids. All the numerical illustrations of wave arrival singularities and their unfolding into pseudo-arrivals are, however, limited to isotropic media. Because of centrosymmetry and time reversal invariance, there are no odd order spatial or time derivatives in the wave equation. By augmenting the classical wave equation with fourth order spatial derivatives, one obtains dispersive corrections to the phase velocity, v, which are quadratic in $\mathbf{k}$. Through suitable Fourier transforms and integration, the characteristic pseudo-wave arrival functions are derived for the different types of wave arrival singularities in 2D and 3D elastodynamic Green's functions of isotropic solids.

II. THE WAVE EQUATION IN GRADIENT ELASTICITY

There is an extensive literature on the modification of the classical elastic wave equation to accommodate the effects of spatial dispersion. A Lagrangian approach, based on Hamilton's action principle, is advantageous from several points of view. It provides a convenient means for handling physical and tensor permutation symmetries, for deriving balance (continuity) equations, and for maintaining self-consistency. The Lagrangian envisaged here is for an unconstrained centrosymmetric solid of density ρ undergoing infinitesimal Cartesian displacements u_i. It is time independent and displays time reversal and translational invariance. The kinetic energy term is quadratic in the particle velocities and the potential energy term is quadratic in the first, second and third displacement gradients. As shown by DiVincenzo,[19] Hamilton's action principle applied to this Lagrangian yields, through the the Euler-Lagrange equations, the wave equation

$$\rho\frac{\partial^2 u_i}{\partial t^2} = C_{ijkl}\frac{\partial^2 u_k}{\partial x_j \partial x_l} + E_{ijklmn}\frac{\partial^4 u_k}{\partial x_l \partial x_m \partial x_n \partial x_j}, \tag{1}$$

where the material tensors C_{ijkl} and E_{ijklmn} represent the normal and dispersive elastic constants. The convention of summation over repeated indices applies, with the indices running from 1 to 3.

The fourth order spatial derivatives in this equation at long wavelengths lead to dispersive corrections to the phase velocity, which are quadratic in $k=|\mathbf{k}|$. The absence of third order spatial derivatives is due to the assumed centrosymmetry. Linear spatial dispersion, which occurs along acoustic axes in crystals belonging to certain symmetry classes lacking a center of inversion, has attracted considerable attention in the past,[20–22] but will not be discussed in this paper. Since this paper deals only with weak dispersion, i.e., the first onset of dispersion with decreasing wavelength, higher order derivatives than fourth need not be considered. Metrikine and Askes[23] have shown that the instability or infinite speed of energy propagation implied by Eq. (1) for very large k, can be eliminated by the inclusion of suitable higher order mixed space-time derivatives, but at the cost of abandoning the literal interpretation of u_i as the particle displacement field of the medium. This is an unnecessary complication for the puposes of the present investigation, which is concerned with weak spatial dispersion.

Plane wave solutions of the wave equation: Equation (1) admits plane wave solutions of the form

$$u_i = U_i \exp i(\mathbf{k}\cdot\mathbf{x} - \omega t), \tag{2}$$

with the polarization vector, $\mathbf{U}=(U_i)$, wave vector, $\mathbf{k}=(k_i)$, and angular frequency, $\omega=2\pi f$, being subject to

$$\{C_{ijkl}k_l k_j - E_{ijklmn}k_l k_m k_n k_j - \rho\omega^2\delta_{ik}\}U_k = 0. \tag{3}$$

The corresponding secular equation

$$\det|C_{ijkl}k_l k_j - E_{ijklmn}k_l k_m k_n k_j - \rho\omega^2\delta_{ik}| = 0, \tag{4}$$

represents the dispersion relation for the medium. For given $\mathbf{k}$, there are three eigenfrequencies, $\omega_{\mathbf{k}j}$, and associated polarization vectors, $\mathbf{U}^{\mathbf{k}j}=(U_i^{\mathbf{k}j})$, corresponding to the quasilongitudinal (L) and two quasitransverse (T) modes. The secular equation can be cast in the form of an equation for the phase velocity $v=\omega/k$ by dividing each entry in the determinant by k^2, yielding

$$\det|(C_{ijkl} - k^2 E_{ijklmn}n_m n_n)n_l n_j - \rho v^2\delta_{ik}| = 0, \tag{5}$$

where $\mathbf{n}=\mathbf{k}/k$ is the wave normal.

Since dispersion is being treated as a small correction to the wave equation, one is entitled to carry out the following truncated expansions in powers of k:

$$v_{\mathbf{k}j} = v_{\mathbf{n}j}(1 - \gamma_{\mathbf{n}j}k^2), \tag{6}$$

and

$$\omega_{\mathbf{k}j} = v_{\mathbf{n}j}k(1 - \gamma_{\mathbf{n}j}k^2), \tag{7}$$

where $v_{\mathbf{n}j}$ is the branch and direction dependent phase velocity in the long wavelength limit. The dispersion coefficient, $\gamma_{\mathbf{n}j}$, while depending on branch and direction, is equal in order of magnitude to $(\Lambda/2\pi)^2$, where Λ is the natural length scale of the medium. For example, in the case of a monatomic chain with lattice spacing a and nearest neighbour force constant only, $\gamma = a^2/24$, implying length scale $\Lambda = (\pi/\sqrt{6})a = 1.28a$. All the results in this paper are valid only insofar as dispersion can be regarded as a perturbation, i.e., where $|\gamma_{\mathbf{n}j}|k^2 \ll 1$, and hence they only apply to wavelengths and distances larger than Λ, and to time intervals longer than Λ/v. Attempting to push the results in this paper beyond their domain of validity is to court trouble, with e.g. frequencies becoming imaginary. Because of the limited frequency domain considered, there are no rigid constraints in the form of Kramers-Kronig-type relations on the materials tensors.

Whilst it is common to find dispersion relations ω vs k for solids curving downwards, corresponding to $\gamma_{\mathbf{n}j}$ positive, this is not universally the case. In crystal lattices, the second and more remote neighbour force constants have a stronger influence on $\gamma_{\mathbf{n}j}$ than on $v_{\mathbf{n}j}$, and if some of these constants are negative, this can change the sign of $\gamma_{\mathbf{n}j}$ without causing the lattice to become unstable. In an anisotropic solid, $\gamma_{\mathbf{n}j}$ may be positive in some directions and negative in others. The numerical illustrations for isotropic solids provided below, are for both positive and negative $\gamma_{\mathbf{n}j}$.

III. POINT FORCE GREEN'S FUNCTIONS $G_{kp}(\mathbf{x},t)$ FOR AN INFINITE 3D DISPERSIVE SOLID

The 3D elastodynamic Green's function $G_{kp}(\mathbf{x},t)$ is defined as the x_kth component of the displacement response of an infinite, dispersive anisotropic solid to a unit point force in the x_p direction acting at the origin $\mathbf{x}=0$, and having unit step function time dependence $\Theta(t)$. As such, it has units of displacement divided by force, and is governed by the equation

$$\left(\rho\delta_{ik}\frac{\partial^2}{\partial t^2} - C_{ijkl}\frac{\partial^2}{\partial x_j \partial x_l} - E_{ijklmn}\frac{\partial^4}{\partial x_l \partial x_m \partial x_n \partial x_j}\right)G_{kp}(\mathbf{x},t) = \delta(\mathbf{x})\Theta(t)\delta_{ip}. \tag{8}$$

The set of Green's functions $G_{kp}; k,p = 1,2,3$ form a second rank tensor.

The formal solution of (8) is readily obtained by integral transform methods. A similar procedure is followed here to that used by Every and Kim.[24] On carrying out a quadruple space-time Fourier transform on Eq. (8) one obtains

$$\mathcal{L}_{ik}(\mathbf{k},\omega)G_{kp}(\mathbf{k},\omega) = \frac{i}{\omega + i\varepsilon}\delta_{ip}, \tag{9}$$

where

$$\mathcal{L}_{ik}(\mathbf{k},\omega) = C_{ijkl}k_l k_j - E_{ijklmn}k_l k_m k_n k_j - \rho\omega^2\delta_{ik}. \tag{10}$$

Invoking the spectral resolution theorem, which amounts to diagonalizing the operator $\mathcal{L}_{ik}(\mathbf{k},\omega)$, allows one to write the solution of (9) as

$$G_{kp}(\mathbf{k},\omega) = \frac{-i}{\rho(\omega + i\varepsilon)}\sum_{j=1}^{3}\frac{\Lambda_{kp}^{\mathbf{k}j}}{\omega^2 - (\omega_{\mathbf{k}j})^2}, \tag{11}$$

where

$$\Lambda_{kp}^{\mathbf{k}j} = U_k^{\mathbf{k}j}U_p^{\mathbf{k}j}. \tag{12}$$

On carrying out the inverse Fourier transform one obtains the integral representation

$$G_{kp}(\mathbf{x},t) = \frac{-i}{(2\pi)^4\rho}\int d^3k \exp i\mathbf{k}\cdot\mathbf{x} \times \sum_{j=1}^{3}\int_{-\infty}^{\infty}\frac{d\omega\Lambda_{kp}^{\mathbf{k}j}\exp(-i\omega t)}{(\omega + i\varepsilon)(\omega - \omega_{\mathbf{k}j})(\omega + \omega_{\mathbf{k}j})} \tag{13}$$

for G_{kp}.

The integral with respect to ω is evaluated by means of the Cauchy residue theorem, moving the poles at $\pm\omega_{\mathbf{k}j}$ slightly below the real axis. For $t<0$ the integration contour is completed in the upper half complex plane and the result is zero, since no poles are enclosed. For $t>0$ the contour is completed in the lower half complex plane and the result is

$$G_{kp}(\mathbf{x},t) = \frac{\Theta(t)}{(2\pi)^3\rho}\int d^3k \exp i\mathbf{k}\cdot\mathbf{x}\sum_{j=1}^{3}\frac{\Lambda_{kp}^{\mathbf{k}j}}{(\omega_{\mathbf{k}j})^2}(1 - \cos(\omega_{\mathbf{k}j}t)). \tag{14}$$

In performing the integration with respect to $\mathbf{k}$, it is convenient to orient the k_3 axis in the direction of $\mathbf{x}$, and transform to spherical polar coordinates (k,θ,ϕ), whereby $\mathbf{k}\cdot\mathbf{x} = kx\cos\theta$. The oscillatory part of the integrand, $\exp i\mathbf{k}\cdot\mathbf{x}(1 - \cos(\omega_{\mathbf{k}j}t))$, is much more rapidly varying than the remaining factor, $\Lambda_{kp}^{\mathbf{k}j}/(\omega_{\mathbf{k}j})^2$, and so dispersion is taken account of in the former using Eq. (7) for $\omega_{\mathbf{k}j}$, but the latter factor is approximated by its dispersionless limit, $\Lambda_{kp}^{\mathbf{n}j}/(kv_{\mathbf{n}j})^2$. The integration with respect to k is facilitated by taking its limits to be $-\infty$ and ∞, rather than 0 and ∞, and to compensate, the angular integral is taken over the forward hemisphere only, for which the integration limits for θ are 0 and $\pi/2$, yielding

$$G_{kp} = \frac{\Theta(t)}{8\pi^2\rho}\sum_{j=1}^{3}\left\{\frac{1}{x}\int_0^{2\pi} d\phi\left(\frac{\Lambda_{kp}^{\mathbf{n}j}}{(v_{\mathbf{n}j})^2}\right)_{\theta=\pi/2} - \int_0^{2\pi} d\phi\int_0^{\pi/2}\sin\theta d\theta\frac{\Lambda_{kp}^{\mathbf{n}j}}{(v_{\mathbf{n}j})^2}\frac{1}{(3v_{\mathbf{n}j}|\gamma_{\mathbf{n}j}|t)^{1/3}} \times \mathrm{Ai}\left(\frac{\mathrm{sgn}(\gamma_{\mathbf{n}j})(x\cos\theta - v_{\mathbf{n}j}t)}{(3v_{\mathbf{n}j}|\gamma_{\mathbf{n}j}|t)^{1/3}}\right)\right\}. \quad (15)$$

where $\mathrm{Ai}(z)$ is the Airy function.

The dispersionless classical continuum response is obtained by shrinking the length scale to zero. Using the identity (which is one of the representations for the delta function)

$$\lim_{\gamma_{\mathbf{n}j}\to 0}\frac{1}{(3v_{\mathbf{n}j}|\gamma_{\mathbf{n}j}|t)^{1/3}}\mathrm{Ai}\left(\frac{\mathrm{sgn}(\gamma_{\mathbf{n}j})(x\cos\theta - v_{\mathbf{n}j}t)}{(3v_{\mathbf{n}j}|\gamma_{\mathbf{n}j}|t)^{1/3}}\right) = \delta(x\cos\theta - v_{\mathbf{n}j}t), \quad (16)$$

one obtains

$$G_{kp} = \frac{\Theta(t)}{8\pi^2\rho}\sum_{j=1}^{3}\left\{\frac{1}{x}\int_0^{2\pi} d\phi\left(\frac{\Lambda_{kp}^{\mathbf{n}j}}{(v_{\mathbf{n}j})^2}\right)_{\theta=\pi/2} - \int_0^{2\pi} d\phi\int_0^{\pi/2}\sin\theta d\theta\frac{\Lambda_{kp}^{\mathbf{n}j}}{(v_{\mathbf{n}j})^3}\delta\left(\frac{1}{v_{\mathbf{n}j}}x\cos\theta - t\right)\right\}. \quad (17)$$

Equation (17) is a common starting point for the numerical evaluation of elastodynamic Green's functions of dispersionless anisotropic solids.[24] The first term represents the static Green's function, whilst the second term, which vanishes for $t > x/v_{\mathbf{n}j}$, yields the time dependence of the response. On pulling back from the limit $\gamma_{\mathbf{n}j}=0$, dispersion affects only the second term through the replacement of the delta function by its Airy function counterpart.

The time dependence of $G_{kp}(\mathbf{x},t)$ in the dispersionless limit is punctuated by singularities known as wave arrivals. These arise in the integration over $\mathbf{n}$ in the vicinity of points where $(1/v_{\mathbf{n}j})x\cos\theta$ is stationary, which in the case of an isotropic solid is where $\cos\theta=1$. Well away from wave arrivals, the weak dispersion considered here has minimal effect on the response, which can therefore be calculated using (17). In the vicinity of the wave arrivals, however, the effects of dispersion are pronounced, and the evaluation of (15) is required.

For a general anisotropic solid, the angular integrals in (15) or (17) require numerical methods for their evaluation, but for an isotropic solid these integrals can be done analytically. From this point on the discussion of the 3D Green's function is tailored to isotropic solids.

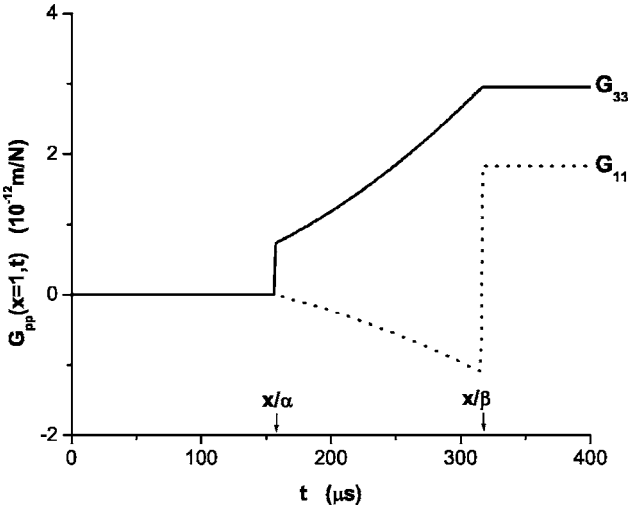

FIG. 1. Point force Green's functions G_{11} and G_{33} for isotropic polycrystalline aluminium in the absence of dispersion.

IV. GREENS' FUNCTION $G_{kp}(x,t)$ FOR AN ISOTROPIC SOLID

In the case of an isotropic solid there are only two independent components of the Green's tensor to consider, namely, G_{33} and $G_{11}=G_{22}$, all the other components being zero. The SH mode, i.e., the transverse mode polarized in the x_1x_2 plane, does not contribute to G_{33}, only the L mode and SV (sagitally polarized transverse) mode do. $\mathbf{U}^{\mathbf{n}L}$ is parallel to $\mathbf{n}$ and so $\Lambda_{33}^{\mathbf{n}L}=\cos^2\theta$, while $\Lambda_{33}^{\mathbf{n}T}=\sin^2\theta$ for the SV mode. Away from the wave arrivals, where the effects of dispersion are minimal, the integrations over θ and ϕ in Eq. (15) can be done analytically, and yield

$$G_{33}(x,t) = \frac{\Theta(t)}{4\pi\rho x}\left\{\frac{1}{\beta^2}\Theta\left(\frac{\beta t}{x}-1\right) + \frac{t^2}{x^2}\left[\Theta\left(\frac{\alpha t}{x}-1\right) - \Theta\left(\frac{\beta t}{x}-1\right)\right]\right\}, \quad (18)$$

where $x=x_3$, $\alpha=v_{\mathbf{n}}^L$, and $\beta=v_{\mathbf{n}}^T$. In the calculation of G_{11} all three modes contribute, and the result is

$$G_{11}(x,t) = \frac{\Theta(t)}{8\pi\rho x}\left\{\frac{1}{\alpha^2}\Theta\left(\frac{\alpha t}{x}-1\right) + \frac{1}{\beta^2}\Theta\left(\frac{\beta t}{x}-1\right) - \frac{t^2}{x^2}\left[\Theta\left(\frac{\alpha t}{x}-1\right) - \Theta\left(\frac{\beta t}{x}-1\right)\right]\right\}. \quad (19)$$

Equations (18) and (19) are consistent with Eq. (4.23) of Aki and Richards.[1] G_{33} and G_{11}, calculated for aluminium in the absence of dispersion, and for $x=1m$ are shown in Fig. 1.

The step functions in (18) and (19) emerge from the $\theta=0$ cutoff in the integrations. They propagate the wave arrival singularities in G_{pp}, i.e., the conspicuous kinks and discontinuities in Fig. 1. The L wave arrival propagates at the longitudinal speed α, and with the polarization of this mode

being in the x_3 direction, the arrival takes the form of a discontinuity [step function $\Theta(\tau)$, τ=time after arrival] in G_{33} and a kink [ramp function $R(\tau)$] in G_{11}. The T arrival, propagating at the transverse velocity β, and because the polarization is perpendicular to the x_3 direction, takes the form of a discontinuity in G_{11} and a kink in G_{33}. The Green's function $G^{\delta}_{pp}(x,t)$ pertaining to a point impulse, is the time derivative of $G_{pp}(x,t)$ above, and its wave arrivals take the form of $\delta(\tau)$ and $\Theta(\tau)$ singularities.

V. EFFECT OF DISPERSION ON WAVE ARRIVALS: QUASIARRIVALS

The wave arrivals treated above are singular in form because dispersion has been neglected. Incorporation of dispersion leads to the unfolding of wave arrivals into characteristic wave trains. The step function, delta function and ramp function arrivals are treated below. For a well developed unfolding to occur requires that $x \gg \Lambda$, where $\Lambda = 2\pi\sqrt{|\gamma|}$ is the natural length scale for the medium. The small parameter for the analysis below is accordingly $\eta = \Lambda/x$.

A. Unfolding of the step function arrival

For this purpose, the L arrival in $G_{33}(x,t)$ is considered. In the vicinity of the L arrival at $t_0 = x/\alpha$, the SV contribution to $G_{33}(x,t)$, obtained from (17), is equal to $1/4\pi\rho\alpha^2 x$, and displays no singular behavior. The L mode contribution obtained from (15) is

$$G_{33}(x,\tau) = \frac{1}{4\pi\rho\alpha^2}\left\{\frac{1}{x} - \int_0^1 du \frac{u^2}{(3|\gamma|x)^{1/3}} \times \mathrm{Ai}\left(\frac{\mathrm{sgn}(\gamma)(x(u-1)-\alpha\tau)}{(3|\gamma|x)^{1/3}}\right)\right\}, \quad (20)$$

where $\gamma = \gamma_{\mathbf{n}L}$, $u = \cos\theta$, and $\tau = t - t_0$, $|\tau| \ll t_0$. Because $x/(3|\gamma|x)^{1/3} \gg 1$, the Airy function in the integrand falls off rapidly as u recedes from 1, and negligible error is incurred by replacing the lower limit of the integral by $-\infty$ and the factor u^2 by 1. With the further substitutions

$$p = \frac{(x(u-1)-\alpha\tau)}{(3|\gamma|x)^{1/3}}$$

and

$$T = \frac{\alpha\tau}{(3|\gamma|x)^{1/3}} = \left(\frac{4\pi^2}{3}\right)^{1/3}\frac{\tau}{\tau_0},$$

where $\tau_0 = t_0\eta^{2/3}$, one obtains

$$4\pi\rho\alpha^2 x G_{33}(x,\tau) = \Psi_\Theta(T) = \int_{-T}^{\infty} dp\ \mathrm{Ai}(\mathrm{sgn}(\gamma)p). \quad (21)$$

There are two characteristic times in the above analysis, t_0, which is the arrival time for the undispersed waveform, and $\tau_0 \ll t_0$, which represents the time scale for the unfolding. Figure 2 depicts the unfolding function $\Psi_\Theta(T)$ and its undispersed counterpart $\Theta(T)$. For $\gamma > 0$, the first maximum of $\Psi_\Theta(T)$ occurs at $T = 2.34$, which corresponds to time and spatial separations from the undispersed wavefront, $\Delta t = 0.99\tau_0 \approx t_0\eta^{2/3}$ and $\Delta x \approx x\eta^{2/3}$, respectively. The precursor, i.e., the initial rise of the displacement preceding the arrival, is analogous to the shadow zone of an edge diffraction pattern, a forbidden zone in the ray approximation. Its presence in the unfolded waveform implies signal propagation at a velocity greater than the limiting velocity α. Not too much significance should be attached to this apparent anomaly, however, since in this zone $\Psi_\Theta(T)$ falls off exponentially, and the first measurable signal leads the arrival by no more than about $\Delta x \approx x\eta^{2/3}$, and thus travels at a velocity $v \approx \alpha(1+\eta^{2/3})$. For small η this velocity will be difficult to distinguish from α. Similar remarks can be made for the shadow zone of the other quasi-arrivals discussed below.

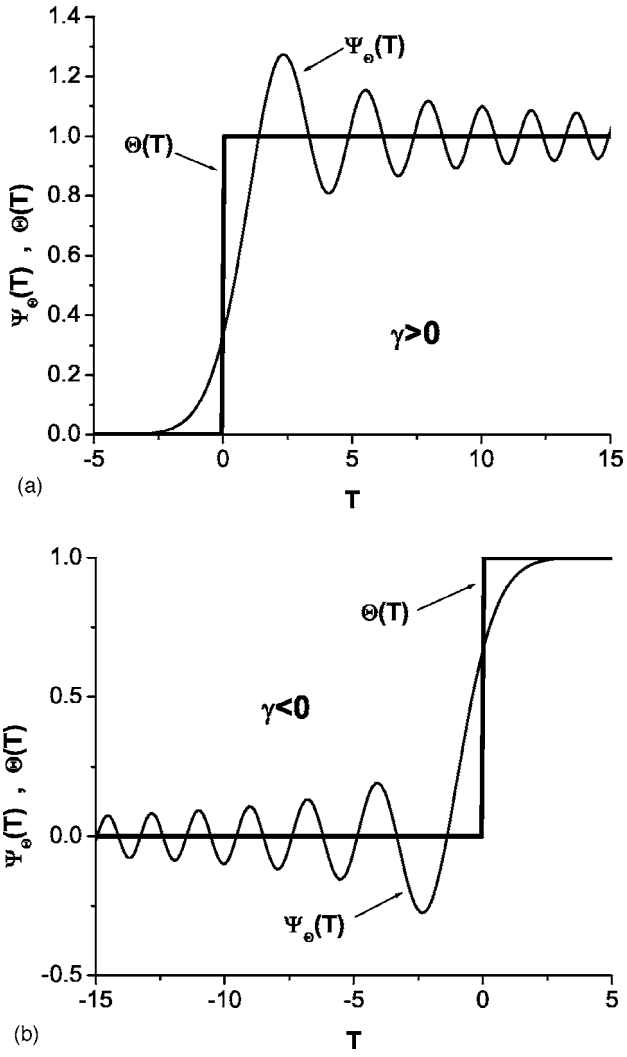

FIG. 2. Unfolding of the $\Theta(T)$ arrival for (a) positive and (b) negative γ.

B. Unfolding of the delta function arrival

The L arrival in $G^{\delta}_{33}(x,t)$ is in the form of a delta function, and its unfolding is obtained by differentiating (21) with respect to time, i.e.,

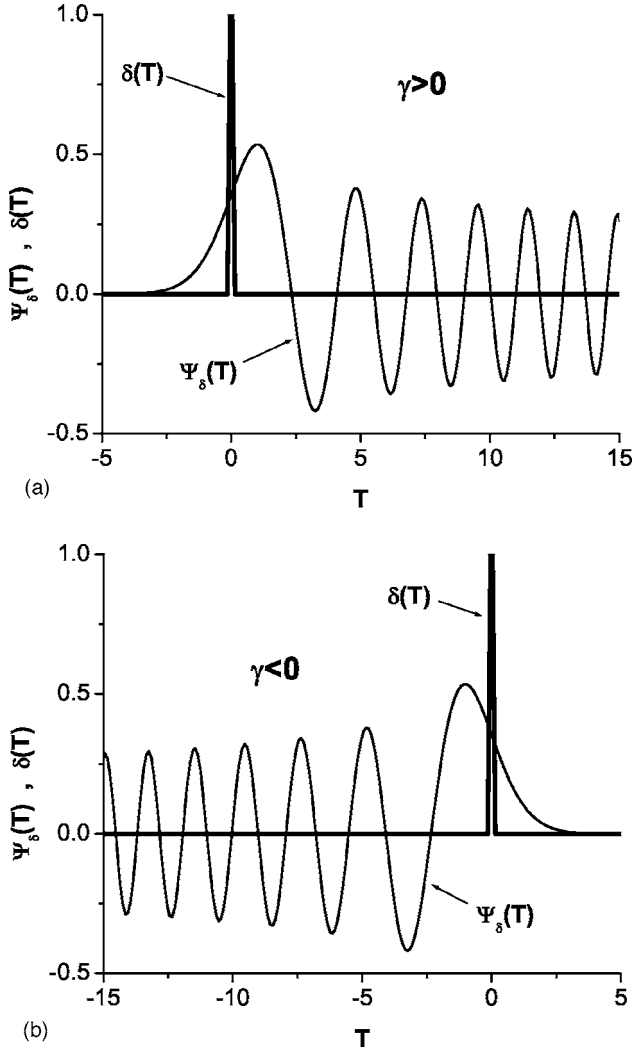

FIG. 3. Unfolding of the $\delta(T)$ arrival for (a) positive (b) and negative γ.

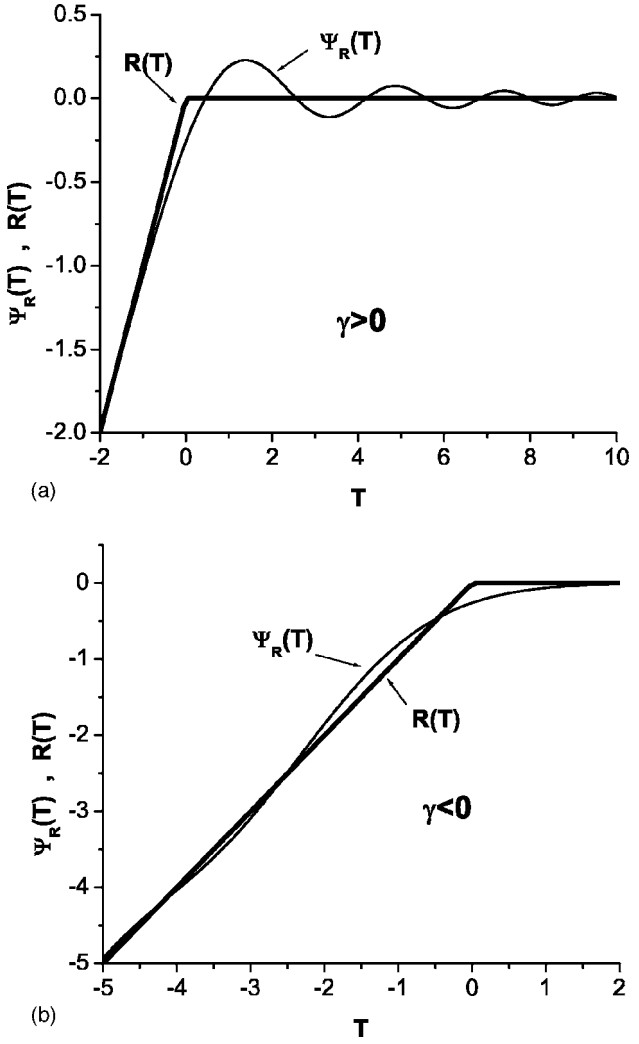

FIG. 4. Unfolding of the $R(T)$ arrival for (a) positive and (b) negative γ.

$$4\pi\rho\alpha x(3|\gamma|x)^{1/3}G_{33}^{\delta}(x,\tau) = \Psi_{\delta}(T) = \mathrm{Ai}(-\mathrm{sgn}(\gamma)T). \tag{22}$$

Figure 3 depicts the unfolding $\Psi_{\delta}(T)$ and its undispersed counterpart $\delta(T)$.

C. Unfolding of the ramp function arrival

For this purpose the T arrival in $G_{33}(x,t)$ is considered. The L mode does not contribute to $G_{33}(x,t)$ in the vicinity of the T arrival at $t=x/\beta$. Near this arrival the dominant term in $G_{33}(x,t)$ is

$$G_{33}(x,\tau) = \frac{-1}{4\pi\rho\beta^2}\int_{-\infty}^{1} du \frac{2(1-u)}{(3|\gamma|x)^{1/3}}\,\mathrm{Ai}\left(\frac{\mathrm{sgn}(\gamma)(x(u-1)-\beta\tau)}{(3|\gamma|x)^{1/3}}\right), \tag{23}$$

where $\gamma=\gamma_{\mathbf{n}T}$ and $\tau=t-(x/\beta)$. As before, the main contribution to the integral is from near the upper limit $u=1$, and so the lower limit has been replaced by $-\infty$, and the factor $1-u^2$ arising from the $\sin^2\theta$ factor, replaced by $2(1-u)$. With the further substitutions

$$p = \frac{(x(u-1)-\beta\tau)}{(3|\gamma|x)^{1/3}}$$

and

$$T = \frac{\beta\tau}{(3|\gamma|x)^{1/3}},$$

one obtains

$$\frac{2\pi\rho\beta^2x^2}{(3|\gamma|x)^{1/3}}G_{33}(x,\tau) = \Psi_R(T) = T - \int_{-T}^{\infty} dp(p+T)\mathrm{Ai}(\mathrm{sgn}(\gamma)p). \tag{24}$$

Figure 4 depicts the unfolding $\Psi_R(T)$ and its undispersed counterpart, $R(T)$. The T arrival of $G_{33}^{\delta}(x,t)$ is in the form of a step function, which has already been discussed.

VI. LINE FORCE GREEN'S FUNCTION $G_{kp}(\mathbf{x},t)$ FOR AN INFINITE DISPERSIVE SOLID

The line force elastodynamic Green's function $G_{kp}(\mathbf{x},t)$ is defined as the x_kth component of the displacement response of an infinite, dispersive anisotropic solid to an impulsive force acting in the x_p direction and distributed with unit line density along the x_3 axis. The (x_1,x_2) plane will be supposed a material's symmetry plane, and only the tensor components $k,p=1,2$ of G_{kp} will be considered. This is a plane strain problem, with force and displacement confined to the (x_1,x_2) plane, and independent of x_3. The antiplane strain problem involved in the calculation of G_{33} will not be treated here, but follows along similar lines. $G_{kp}(\mathbf{x},t)$ can be regarded as the Green's function tensor for a 2D solid. It has units of displacement divided impulse per unit length, and is governed by the equation

$$\left(\rho\delta_{ik}\frac{\partial^2}{\partial t^2}-C_{ijkl}\frac{\partial^2}{\partial x_j\partial x_l}-E_{ijklmn}\frac{\partial^4}{\partial x_l\partial x_m\partial x_n\partial x_j}\right)G_{kp}(\mathbf{x},t)=\delta(\mathbf{x})\delta(t)\delta_{ip}, \tag{25}$$

where the indices run over the values 1 and 2.

Carrying out a triple space-time Fourier transform on (25) yields

$$\mathcal{L}_{ik}G_{kp}=\delta_{ip}, \tag{26}$$

with $\mathcal{L}_{ik}(\mathbf{k},\omega)$ being given by (10), and $\mathbf{k}=(k_1,k_2)$. The solution of (26) is

$$G_{kp}(\mathbf{k},\omega)=-\frac{1}{\rho}\sum_{j=1}^{2}\frac{\Lambda_{kp}^{\mathbf{k}j}}{\omega^2-(\omega_{\mathbf{k}j})^2}. \tag{27}$$

The branch summation extends over the quasi L and quasi T modes polarized in the (x_1,x_2) plane. The pure T mode, polarized in the x_3 direction features only in the calculation of G_{33}.

On carrying out the inverse Fourier transform one obtains the integral representation

$$G_{kp}(\mathbf{x},t)=\frac{-1}{(2\pi)^3\rho}\int d^2k\exp i\mathbf{k}\cdot\mathbf{x}\times\sum_{j=1}^{2}\int_{-\infty}^{\infty}d\omega\frac{\Lambda_{kp}^{\mathbf{k}j}}{(\omega-\omega_{\mathbf{k}j})(\omega+\omega_{\mathbf{k}j})}\exp(-i\omega t), \tag{28}$$

for G_{kp}. As before, the integral with respect to ω is evaluated by means of the Cauchy residue theorem, yielding

$$G_{kp}(\mathbf{x},t)=\frac{\Theta(t)}{(2\pi)^2\rho}\int d^2k\exp i\mathbf{k}\cdot\mathbf{x}\sum_{j=1}^{2}\frac{\Lambda_{kp}^{\mathbf{k}j}\sin(\omega_{\mathbf{k}j}t)}{\omega_{\mathbf{k}j}}. \tag{29}$$

For $x\gg\Lambda$, and limiting the integration to the domain $k\ll 2\pi/\Lambda$, it follows that

$$\frac{\Lambda_{kp}^{\mathbf{k}j}}{\omega_{\mathbf{k}j}}=\frac{\Lambda_{kp}^{\mathbf{k}j}}{kv_{\mathbf{n}j}(1-\gamma_{\mathbf{n}j}k^2)}\approx\frac{\Lambda_{kp}^{\mathbf{n}j}}{kv_{\mathbf{n}j}}, \tag{30}$$

and thus

$$G_{kp}(\mathbf{x},t)=\frac{\Theta(t)}{(2\pi)^2\rho}\sum_{j=1}^{2}\int d^2k\frac{\Lambda_{kp}^{\mathbf{n}j}}{kv_{\mathbf{n}j}}\exp(i\mathbf{k}\cdot\mathbf{x})\times\sin(v_{\mathbf{n}j}(1-\gamma_{\mathbf{n}j}k^2)kt). \tag{31}$$

As with the 3D Green's function, dispersion has been retained in the oscillatory part of the integrand, but not in the more slowly varying remaining factor. In the dispersionless limit, $\gamma_{\mathbf{n}j}\to 0$, and (31) reduces to

$$G_{kp}(\mathbf{x},t)=\frac{\Theta(t)}{(2\pi)^2\rho}\sum_{j=1}^{2}\int d^2k\frac{\Lambda_{kp}^{\mathbf{n}j}}{kv_{\mathbf{n}j}}\exp(i\mathbf{k}\cdot\mathbf{x})\sin(v_{\mathbf{n}j}kt). \tag{32}$$

There is an extensive literature on the evaluation of (32) for anisotropic solids, using techniques such as the Cagniard-de Hoop method and the calculus of residues.[25] Below, isotropic solids are treated, for which (32) can be evaluated analytically, and (31) partially so.

VII. GREEN'S FUNCTION $G_{pp}(x,t)$ FOR AN ISOTROPIC SOLID

For an isotropic solid only the diagonal components of the Green's tensor G_{kp} given by (31) are nonzero. Consider G_{22}, the case of force, component of displacement response and observation point $\mathbf{x}$ all lying in the x_2 direction. On transforming to polar coordinates $(k_1,k_2)\to(k\sin\theta,k\cos\theta)$, and using the fact that $\Lambda_{22}^{\mathbf{n}L}=\cos^2\theta$ and $\Lambda_{22}^{\mathbf{n}T}=\sin^2\theta$, and carrying out the integration with respect to θ, with the limits being 0 and 2π, one obtains

$$G_{22}(x,t)=\frac{\Theta(t)}{2\pi\rho}\left\{\frac{1}{\alpha}\int_0^\infty dk\left[J_0(kx)-\frac{J_1(kx)}{kx}\right]\sin(k\alpha(1-\gamma_Lk^2)t)+\frac{1}{\beta}\int_0^\infty dk\left[\frac{J_1(kx)}{kx}\right]\sin(k\beta(1-\gamma_Tk^2)t)\right\}, \tag{33}$$

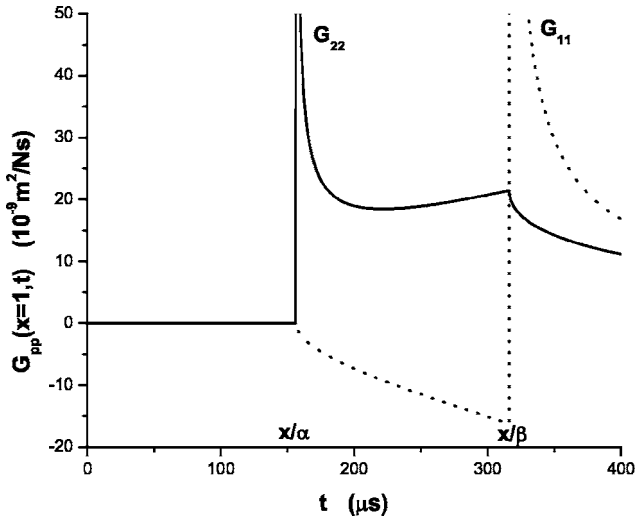

FIG. 5. Line force Green's functions G_{11} and G_{22} for isotropic polycrystalline aluminium in the absence of dispersion.

where $J_n(z)$ are Bessel functions of the first kind, and $\gamma_L = \gamma_{\mathbf{n}L}$, and $\gamma_T = \gamma_{\mathbf{n}T}$. Note that the limits on the integration with respect to k are 0 and $^{\infty}$, not $^{-\infty}$ and $^{\infty}$ as in the case of the 3D Green's function. G_{11} is given by a similar expression to (33), but with the factors in the square brackets interchanged.

Well away from the wave arrivals at $t=x/\alpha$ and $t=x/\beta$ the effects of dispersion are negligible, and $G_{22}(x,t)$ can be evaluated by setting $\gamma_L=\gamma_T=0$. On performing the integration with respect to k, one obtains

$$G_{22}(x,t) = \frac{\Theta(t)}{2\pi\rho x}\left\{ \frac{\frac{1}{\alpha}\left(\frac{\alpha t}{x}\right)^2 \Theta\left(\frac{\alpha t}{x}-1\right)}{\sqrt{\left(\frac{\alpha t}{x}\right)^2 - 1}} - \frac{1}{\beta}\sqrt{\left(\frac{\beta t}{x}\right)^2 - 1}\,\Theta\left(\frac{\beta t}{x}-1\right) \right\}. \tag{34}$$

The calculation of $G_{11}(x,t)$ follows along similar lines, and yields

$$G_{11}(x,t) = \frac{\Theta(t)}{2\pi\rho x}\left\{ -\frac{1}{\alpha}\sqrt{\left(\frac{\alpha t}{x}\right)^2 - 1}\,\Theta\left(\frac{\alpha t}{x}-1\right) + \frac{\frac{1}{\beta}\left(\frac{\beta t}{x}\right)^2 \Theta\left(\frac{\beta t}{x}-1\right)}{\sqrt{\left(\frac{\beta t}{x}\right)^2 - 1}} \right\}. \tag{35}$$

Equations (34) and (35) are consistent with Eq. (7.179) of Achenbach.[7] Figure 5 shows $G_{22}(x,t)$ and $G_{11}(x,t)$ in the absence of dispersion, calculated for polycrystalline aluminium, taking $x=1m$.

For both Green's functions the response is zero until the longitudinal wave arrival at $t=x/\alpha$. At that instant, $G_{22}(x,t)$ displays an infinite discontinuity, while the gradient of $G_{11}(x,t)$ displays an infinite discontinuity. Approaching the arrival from positive values of $\tau=t-x/\alpha$, G_{22} diverges as $1/\sqrt{\tau}$, while G_{11} varies as $-\sqrt{\tau}$. At the transverse wave arrival at $t=x/\beta$, the situation is reversed, and for positive values of $\tau=t-x/\beta$, G_{22} varies as $-\sqrt{\tau}$, while G_{11} diverges as $1/\sqrt{\tau}$. For large values of t, both G_{22} and G_{11} fall off as $1/t$. This is the well-known afterglow effect, and can be interpreted as the response arriving from points at ever increasing distances along the line source.[26]

VIII. DISPERSION OF WAVE ARRIVALS: QUASI-ARRIVALS

As with the 3D Green's functions, incorporation of dispersion results in the unfolding of the wave arrival singularities into characteristic oscillatory wave trains. The small parameter, as before, is $\eta=\Lambda/x$, although to simplify the notation, we will make use of the auxiliary parameter $\hat{\eta} = \eta/2\pi = \sqrt{|\gamma|}/x$. There are two characteristic times, t_0, the undispersed L or T wave arrival time, and $\tau_0 = t_0\eta^{2/3}$ (or $\hat{\tau}_0 = t_0\hat{\eta}^{2/3}$), which represents the time scale for the unfolding.

A. Unfolding of the $1/\sqrt{\tau}$ singularity

For this purpose the L arrival at $t_0=x/\alpha$ in $G_{22}(x,t)$ is considered. The L mode contributes the singular behaviour together with a term proportional to t, which is cancelled by an equal and opposite term contributed by the T mode. In the region of the L arrival, (33) thus reduces to

$$G_{22}(x,t) = \frac{\Theta(t)}{2\sqrt{2}\pi\rho\alpha x\hat{\eta}^{1/3}}\Psi_{-1/2}, \tag{36}$$

where

$$\Psi_{-1/2}(T) = \sqrt{2}\,\hat{\eta}^{1/3}\left\{ 1 + \hat{\eta}^{2/3}T + \int_0^{\infty} dk \left\{ J_0(k) - \frac{J_1(k)}{k} \right\} \times \sin(k(1+\hat{\eta}^{2/3}T)(1-\mathrm{sgn}(\gamma)\,\hat{\eta}^2k^2)) \right\}, \tag{37}$$

$\hat{\eta}=\sqrt{|\gamma_L|}/x$, and $T=(t-t_0)/\hat{\tau}_0$. Both factors in the integrand of (37) are oscillatory, and the consequence is rather slow convergence of the integral. In numerical calculations, to assure convergence within the range of k in which dispersion can be regarded as small (i.e., $\hat{\eta}^2k^2 \leq 0.05$), the integrand has been multiplied by a smooth windowing function

$$W(k) = \tfrac{1}{2}(1+\cos(\pi k/k_{\max})), \tag{38}$$

where $k_{\max}=\sqrt{0.05}/\hat{\eta}$, and the upper limit of the integral taken as $k_{\max}$. Trials with other windowing functions have yielded little difference in the results. A physical interpretation of the windowing function might be that is represents damping that is an increasing function of spatial frequency,

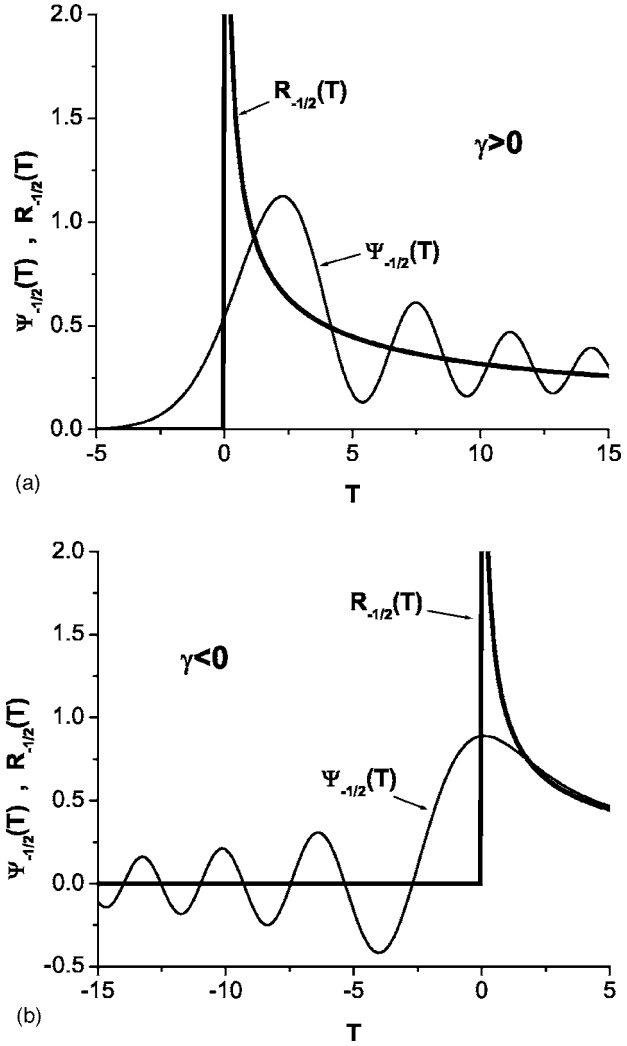

FIG. 6. Unfolding of the $R_{-1/2}(T)$ arrival for (a) positive and (b) negative γ.

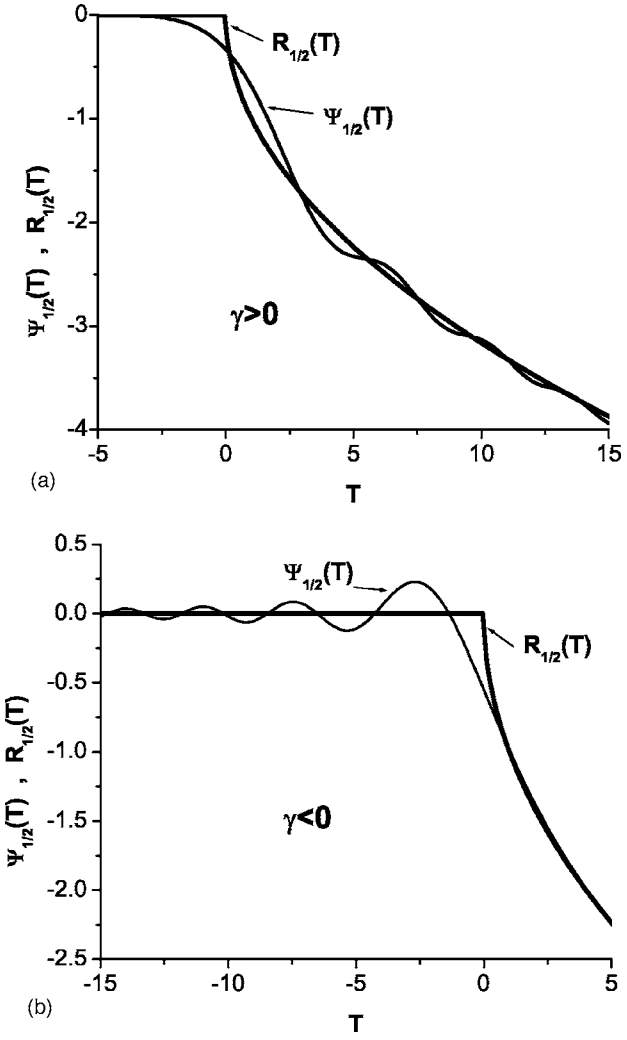

FIG. 7. Unfolding of the $R_{1/2}(T)$ arrival for (a) positive and (b) negative γ.

or the suppression of higher spatial frequencies through some smearing out of the line force.

The unfolding function $\Psi_{-1/2}(T)$, numerically evaluated for $\hat{\eta}=0.0001$ is shown in Fig. 6 for γ $+ve$ and $-ve$, together with its undispersed counterpart

$$R_{-1/2}(T) = \Theta(T)/\sqrt{T}. \tag{39}$$

The result is insensitive to the value of $\hat{\eta}$ for sufficiently small $\hat{\eta}$. The leading factor $\sqrt{2}\hat{\eta}^{1/3}$ in (37) is required to normalize $\Psi_{-1/2}(T)$ to the same mean value as $R_{-1/2}(T)$ for $T>0$. Equations (37) and (39) only hold well for times close to the arrival, i.e., for $\hat{\eta}^{2/3}|T| \ll 1$, and this condition is reasonably well satisfied for the time ranges depicted in Fig. 6. A proper mathematical analysis of the behavior of $\Psi_{-1/2}(T)$, in the limit $\hat{\eta}\to 0$, remains to be done, and the same applies to the function $\Psi_{1/2}(T)$ discussed below.

B. Unfolding of the $-\sqrt{\tau}$ singularity

For this purpose the L mode contribution to $G_{11}(x,t)$ in the region of the L arrival is considered. A similar calculation to that above shows that the unfolded singular part of G_{11} has the form

$$\frac{\Theta(t)\sqrt{2}}{\pi\rho\alpha x\hat{\eta}^{1/3}}\Psi_{1/2},$$

where

$$\Psi_{1/2}(T) = \frac{1}{\sqrt{2}\hat{\eta}^{1/3}}\left\{-(1+\hat{\eta}^{2/3}T) + \int_0^\infty dk\left\{\frac{J_1(k)}{k}\right\} \times \sin(k(1+\hat{\eta}^{2/3}T)(1-\mathrm{sgn}(\gamma)\hat{\eta}^2k^2))\right\}. \tag{40}$$

The unfolding function $\Psi_{1/2}(T)$, numerically evaluated for $\hat{\eta}=0.0001$ is shown in Fig. 7 for γ $+ve$ and $-ve$, together with its undispersed counterpart $R_{1/2}(T)=-\Theta(T)\sqrt{T}$.

IX. DISCUSSION

Wave arrival singularities are a dominant feature in elastodynamic Green's functions, and are all that survive in the

far field, in the sense that most of the wave energy is concentrated near arrivals, the more so with distance of travel. Under the influence of spatial dispersion, which arises when the wavelength approaches the natural length scale of the medium, wave arrival singularities unfold into oscillatory waveforms known as pseudo-wave arrivals. In this paper the unfoldings have been determined for the step, delta and ramp wave arrival singularities in the point force Green's functions of isotropic solids, and the $1/\sqrt{\tau}$ and $-\sqrt{\tau}$ wave arrivals for the line force Green's functions.

For positive dispersion, corresponding to the phase velocity being a decreasing function of spatial frequency, the unfolded wave form rapidly approaches the undispersed wave form for early times, starts deviating from it near the arrival time, reaches a maximum a short time after the arrival, and then oscillates with decreasing amplitude around the undispersed waveform. For negative dispersion, corresponding the phase velocity being an increasing function of spatial frequency, the order is reversed, with the oscillations preceding the arrival.

The results presented here are of a general nature, and are applicable to a wide variety of transient wave phenomena in media exhibiting spatial dispersion, including crystals, fibrous and layered composites and granular and porous solids.

ACKNOWLEDGMENTS

J. D. Kaplunov, G. Rogerson, E. Nolde, and H. J. Maris are thanked for stimulating discussions. Financial support for this research was provided by the South African National Research Foundation under Grant No. 2053311.

*Electronic address: everya@physics.wits.ac.za

[1] K. Aki and P. G. Richards, *Quantitative Seismology*, 2nd ed. (University Science Books, Sausalito, CA, 2002).
[2] A. Ben-Menahem and S. J. Singh, *Seismic Waves and Sources*, 2nd ed. (Dover, Mineola, NY, 1981).
[3] J. W. Tucker and V. W. Rampton, *Microwave Ultrasonics in Solid State Physics* (North-Holland, Amsterdam, 1973).
[4] R. M. Christensen, *Mechanics of Composite Media* (Wiley, New York, 1979).
[5] H.-B. Muhlhaus and F. Oka, Int. J. Solids Struct. **33**, 2841 (1996).
[6] H.-Y. Hao and H. J. Maris, Phys. Rev. B **63**, 224301 (2001).
[7] J. D. Achenbach, *Wave Propagation in Elastic Solids* (North-Holland, Amsterdam, 1993).
[8] J. D. Kaplunov, L. Yu. Kossovich, and E. V. Nolde, *Dynamics of Thin Walled Elastic Bodies* (Academic, San Diego, 1998).
[9] W. Sachse and Y.-H. Pao, J. Appl. Phys. **49**, 4320 (1978).
[10] M. Elices and F. Garcia-Moliner, in *Physical Acoustics*, edited by W. P. Mason (Academic, New York, 1968), Vol. 5, Chap. 4.
[11] H. Askes and A. V. Metrikine, Eur. J. Mech. A/Solids **21**, 573 (2002).
[12] R. D. Mindlin, in *Mechanics of Generalized Continua*, edited by E. Kröner (Springer, Berlin, 1968), p. 312.
[13] J. A. Krumhansl, in *Lattice Dynamics*, edited by R. F. Wallis (Pergamon, Oxford, 1975), p. 627.
[14] *Mechanics of Generalized Continua* (Ref. 12).
[15] R. Lakes, in *Continuum Models for Materials with Microstructure*, edited by H. Muhlhaus (Wiley, New York, 1995), Chap. 1.
[16] A. C. Eringen, Int. J. Eng. Sci. **22**, 1113 (1984).
[17] G. Herrmann and J. D. Achenbach, in *Mechanics of Generalized Continua* (Ref. 12), p. 69.
[18] R. Artan and B. S. Altan, Int. J. Solids Struct. **39**, 5927 (2002).
[19] D. P. DiVincenzo, Phys. Rev. B **34**, 5450 (1986).
[20] D. L. Portigal and E. Burstein, Phys. Rev. **170**, 673 (1968).
[21] A. G. Every, Phys. Rev. B **36**, 1448 (1987).
[22] A. L. Shuvalov and A. G. Every, J. Phys. A **33**, 5105 (2000).
[23] A. V. Metrikine and H. Askes, Eur. J. Mech. A/Solids **21**, 555 (2002).
[24] A. G. Every and K. Y. Kim, J. Acoust. Soc. Am. **95**, 2505 (1994).
[25] C.-Y. Wang and J. D. Achenbach, Wave Motion **16**, 389 (1992).
[26] G. Barton, *Elements of Green's Functions and Propagation* (Clarendon, Oxford, 1989).